frontiers | Frontiers in Ecology and Evolution

TYPE Original Research
PUBLISHED 21 December 2023
DOI 10.3389/fevo.2023.1218658

OPEN ACCESS

EDITED BY
Kunshan Bao,
South China Normal University, China

REVIEWED BY
Zhiwei Wan,
Jiangxi Normal University, China
Kun Zhang,
Huaibei Normal University, China

*CORRESPONDENCE
Bin Xue
Bxue@niglas.ac.cn

RECEIVED 07 May 2023
ACCEPTED 29 November 2023
PUBLISHED 21 December 2023

CITATION
Ling C, Xue B, Yao S, Zhang W, Pan D and Tang L (2023) High-resolution sea-level fluctuations during the Mid-Holocene in the Ningshao Coastal Plain region, eastern China. *Front. Ecol. Evol.* 11:1218658. doi: 10.3389/fevo.2023.1218658

High-resolution sea-level fluctuations during the Mid-Holocene in the Ningshao Coastal Plain region, eastern China

Chaohao Ling[1,2], Bin Xue[2]*, Shuchun Yao[2], Wenchao Zhang[3], Dadong Pan[1] and Lingyu Tang[4]

[1]School of History and Geography, Minnan Normal University, Zhangzhou, China, [2]State Key Laboratory of Lake Science and Environment, Nanjing Institute of Geography and Limnology, Chinese Academy of Sciences, Nanjing, China, [3]School of Earth Sciences and Resources, China University of Geosciences (Beijing), Beijing, China, [4]Nanjing Institute of Geology and Palaeontology, Chinese Academy of Sciences, Nanjing, China

Sea level changes during the Mid-Holocene directly influenced the Neolithic culture in the Yangtze River Delta region (YRD). However, the high-resolution sea level change characteristics for this period remain unclear. In this study, we performed a high-resolution palynological analysis, including pollen, Dinoflagellate cysts, and Foraminiferal organic linings, using a high-resolution sediment core from Shanglin Lake, in the North of Ningshao Plain (the south of Hangzhou Bay). 11 accelerator mass spectrometry ^{14}C(AMS) datings indicate the age of the sediments range from 8 cal ka B.P. to 5.6 cal ka B.P. The results show that during the Mid-Holocene, Shanglin Lake evolved from an estuary – subtidal lagoon – semi-enclosed bay – semi-enclosed lagoon – semi-enclosed bay – enclosed lagoon to a modern freshwater lake. There was a period of no, or minimal, eustatic sea-level rise between 7733 and 7585 cal yr B.P. The Mid-Holocene high sea level comes in 7253–7082 cal yr BP. Between 7000 cal yr BP and 5502 cal yr BP, the sea level is close to modern value. The sea level change during this period had a significant impact on the local Neolithic human activity.

KEYWORDS

Holocene, sea-level fluctuations, pollen, dinoflagellate cysts, foraminiferal organic linings, Ningshao coastal plain

1 Introduction

The cultivation and domestication of crops have been a revolutionary event in human history, and the origin, domestication, and cultivation of rice, a major food source for humans, is one of the major focuses of environmental archaeological investigation (Fuller, 2007; Fuller, 2011; Silva et al., 2015). The middle and lower reaches of the Yangtze River are

densely populated and widely recognized as the birthplace of rice cultivation, and studies on the origin and development of rice cultivation in this region have received increasing attention in the past decades (Zong et al., 2007; Fuller et al., 2009; Zheng et al., 2011; Zong et al., 2011; He et al., 2018; Zheng et al., 2018; Innes et al., 2019; He et al., 2020).

The Mid-Holocene Neolithic culture in the Yangtze River Delta was mainly based on rice agriculture, and it is widely regarded as the core area where rice agriculture originated (Zong et al., 2007; Fuller et al., 2009; Zheng et al., 2011; Silva et al., 2015; Liu et al., 2020), human prehistoric civilization in this region has experienced many ups and downs, and cultural faults have been found in many archaeological sites in the past half century (Zhu et al., 2003; Zhu et al., 2003; He et al., 2018; Wang et al., 2018; He et al., 2020). Rice farming is influenced by many factors such as terrain, climate, soil, and hydrology (Zhu et al., 2003; Zhao, 2010; Zhao, 2019). Which is different from the middle reaches of the Yangtze River, the hydrology change caused by sea level change in the Yangtze River Delta is one of the most important factors (Zong et al., 2011; He et al., 2018; He et al., 2020).

The Yangtze River Delta region experienced dramatic sea-level fluctuations in the Holocene, especially in the Mid-Holocene. In the Ningshao plain of eastern China, sea-level fluctuation during the Mid-Holocene is of particular interest, because it seriously affected the development of Neolithic cultures such as the Majiabang (~7000–6000 cal yr BP), Liangzhu (~5200–4000 cal yr BP), Kuahuqiao (~8000–7200 cal yr BP) and the Hemudu (~7000–5000 cal yr BP) cultures around the Hangzhou Bay area (Chen and Stanley, 1998; Sandweiss, 2003; Zong, 2004; Zong et al., 2007; Song et al., 2013; Zhu et al., 2003; Liu et al., 2016; Liu et al., 2018; Wang et al., 2018; Tang et al., 2019). However, due to the lack of high-quality chronology-controlled sequences, the sea-level fluctuations during the Mid-Holocene are still poorly cognition. As a result, the cognition of sea level change fluctuation has shown great difference (Wang et al., 2012; Zheng et al., 2018), which made the cultural interruptions were caused by marine transgression or land floods is still in dispute (Chen and Stanley, 1998; Xie and Yuan, 2012; Song et al., 2013; Liu et al., 2016; Liu et al., 2018; Wang et al., 2018; Tang et al., 2019).

In this study, we report pollen, Dinoflagellate cysts, Foraminiferal organic linings, and organic $\delta^{13}C$ analyses from a core collected in the Shanglin Lake located in a low-energy, surrounded by hill, the average altitude of the North of Ningshao Plain is less than 8 m, remote from any significant fluvial source of sediment. Multiple proxy analyses were performed to reconstruct sea level change in the Mid-Holocene to identify the cause of cultural interruptions on the Ningshao Plain.

2 Materials and methods

2.1 Study area and field sampling

The Ningshao Plain is located in a transitional zone between the Mid-subtropical to northern subtropical belts under the influence of the East Asian Monsoon. The region experiences marked seasonality in both temperature and precipitation, with an annual mean temperature of 16.2°C and a mean temperature is ~4°C in January and ~28°C in July, and annual mean precipitation is about 1600 mm (Ningbo Chorography Codification Committee, 1995). This area was covered by mixed evergreen deciduous broad-leaved forest, showing the characteristics of transition from evergreen broad-leaved forest to deciduous broad-leaved forest vegetation. The vegetation in the hills is mainly the masson pine community and Rhododendron community. Masson pine forest is mixed with Chinese fir and broad-leaved trees, showing the appearance of a mixed forest. Dominant plant species include: *Pinus massoniana*, *Aphananthe*, *Castanea*, *Castanopsis sclerophylla*, *Castanopsis*, *Cyclobalanopsis*, *Liquidambar formosana*, *Quercus aliena*, *Quercus acutissima*, *Celtis* and *Ulmus* (Wu, 1980).

Shanglin Lake is located in the Ningshao Coastal Plain area on the south bank of Hangzhou Bay. Its terrain is high in the south and low in the north, and it is spread out towards Hangzhou Bay in the shape of three steps of hills, plains, and tidal flats (Figure 1). Shanglin Lake is located in a low-energy, surrounded by hill (Figure 1), remote from any significant fluvial source of sediment. It is located about 23 kilometers north of Hangzhou Bay. The sediments are valuable archives for the reconstruction of sea-level changes.

There are few studies on the geomorphologic evolution during the Mid-Holocene sea level change in the Cixi area, south bank of Hangzhou Bay. Wang et al. (1982) reconstructed the Holocene sea-level change curve in the coastal areas of Zhejiang by combining hundreds of geomorphological survey cores with coastal stratigraphic sequence, geomorphologic features, and archaeological data. Feng and Wang (1986) further added new materials and dating to reconstruct the coastline in three periods during the Mid-Holocene in this area (Figure 1B).

We chose the lagoon Shanglin Lake located near the ancient coastline (Chen et al., 1984), which is on a hill close to the Tianluoshan site and Hemudu site, etc. (Figure 1B). The lakes in the foothills of this area were dominated by nature at the end of primitive society and were little affected by human activities.

We drilled six exploratory cores (SLH-1-SLH6) on the water platform without sampling using drilling tools in advance to facilitate the mapping of the lake bottom sedimentation and then drilled four cores with a piston seal sampler operated on the water platform according to the drilling. Details of all exploratory cores and cores are shown in Figure 2.

We split all of these cores with 1 cm intervals after completion of drilling in the State Key Laboratory of Lake Science and Environment, Nanjing Institute of Geography and Limnology, Chinese Academy of Sciences, China. After describing the lithology and photographing, we selected 16 samples, including plant fragments, shells, and wood for AMS ^{14}C dating at Beta Analytic Inc. According to the detailed stratigraphic situation (Figure 2 and Table 1) and the dating results of each cores (Table 2), we chose sampling core 18SLH4 as the focus of this paper.

2.2 Grain size testing and analysis

Cores were subsampled at the same intervals from the core for a total of 265 subsamples. These samples were firstly pretreated with

10.3389/fevo.2023.1218658

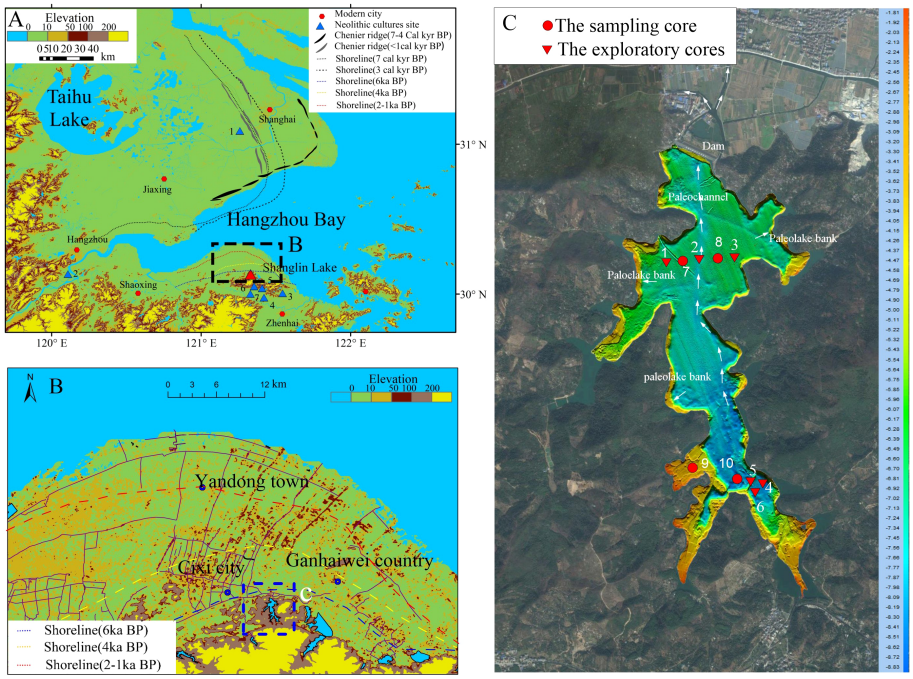

FIGURE 1
The location of the study area and the sample site. **(A)** Location of the study area, both sides of Hangzhou Bay, showing the topography, chenier ridges, and palaeo-shorelines (Wang, 1982; Feng and Wang, 1986). The seven culture sites are: 1 Beiganshan site (Chen et al., 2005; Zong et al., 2011); 2 Kuahuqiao site (Zong et al., 2007; Shu et al., 2010); 3 Yushan site (He et al., 2018; Wang et al., 2018); 4–7 Hemudu (Li et al., 2009; Wang et al., 2018). **(B)** Geographical map showing the present topographic features and the positions of cheniers and palaeo-shorelines during the Mid-Holocene. **(C)** Bottom topography of Shanglin Lake and the cores collected for this study numbered in sequence according to their distance from the Shanglin Lake (Table 1).

10% H_2O_2 and then 10% HCl to remove organic matter and carbonates respectively, and then washed in distilled water to remove residual HCl. Following this, 5 ml of 5% Calgon® (sodium hexametaphosphate) was added to each sample before shaking in an ultrasonic bath for 15 min to prevent flocculation of finegrained particles (Beuselinck et al., 1998). The grain size was measured on each subsample with a Beckman Coulter Laser Diffraction Particle Size Analyzer (Mastersize2000) in the State

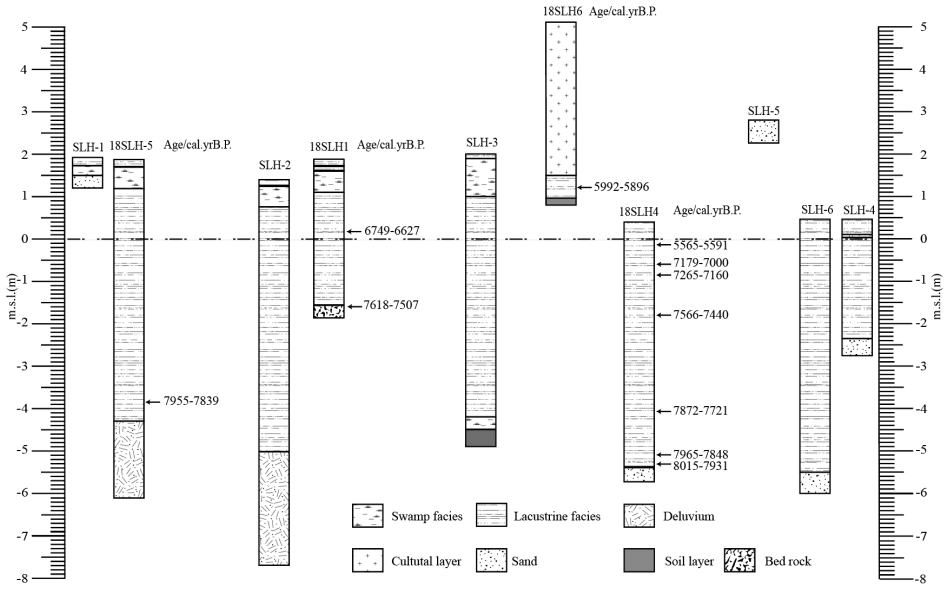

FIGURE 2
Stratigraphic of cores with calibrated mean radiocarbon ages.

TABLE 1 Details of the stratigraphic sequences recorded for all cores.

No.	Cores	Location	Lithological description
1	SLH-1	N 30°08′33.74″ E 121°19′36.11″	0–15 cm. Yellowish–gray clayey silt. Soft lacustrine sediments. 15–40 cm. Bluish gray silty clay. Compact lacustrine sediments. 40–50 cm. Gray dark clayey silt. Compact lacustrine sediments. Below 50 cm. Yellow sand with gravel. Lake bottom sediments.
2	SLH-2	N 30°08′36.86″ E 121°19′49.14″	0–10 cm. Bluish gray clay. Soft lacustrine sediments. 10–60 cm. Yellowish brown clay with plant fragments and roots. Bog sediments. 60–300 cm. Bluish gray silty clay. Compact lacustrine sediments. 300–600 cm. Yellowish–gray clay. A few plant fragments are present in this section. Soft lacustrine sediments. 600–860 cm. The gray–brown mixture of sand and mud. Some plant fragments. Alluvial facies or eluvial facies sediments.
3	SLH-3	N 30°08′36.92″ E 121°19′58.94″	0–11 cm. Bluish gray clay. Soft lacustrine sediments. 11–102 cm. Yellowish brown silty clay. A few plant fragments. Compact bog sediments. 102–625 cm. Bluish gray clayey silt. A few plant fragments. Compact lacustrine sediments. 625–650 cm. Yellowish brown clay. A few plant fragments. Compact bog sediments. 650–690 cm. Yellowish brown and light gray clay. Compact paleosols.
4	SLH-4	N 30°07′49.19″ E 121°20′03.58″	0–280 cm. Bluish gray clayey silt. Soft lacustrine sediments. Bluish gray sand with gravel at 60–70 cm. Bedrock at 280–320 cm.
5	SLH-5	N 30°07′48.62″ E 121°20′02.51″	0–40 cm. Gravel with sand. Unable to sample.
6	SLH-6	N 30°07′46.76″ E 121°20′02.67”	0–60 cm. Bluish gray clayey silt. Lacustrine sediments. Bedrock at 600–650 cm.
7	18SLH1	N 30°08′36.94″ E 121°19′55.40″	0–20 cm. Bluish gray clay. Soft lacustrine sediments. 20–30 cm. Bluish gray clayey silt. Compact lacustrine sediments. 30–80 cm. Yellowish–gray silty clay. A few plant fragments. 80–140 cm. Bluish gray clayey silt. A few plant fragments. Compact lacustrine sediments. 140–350 cm. Bluish gray clayey silt. Soft lacustrine sediments. Abundant shell fragments at 350 cm. Bedrock at 360–380 cm.
8	18SLH4	N30°07’46.71” E121°20’0.28”	0–22 cm. Yellowish–gray clay. Soft lacustrine sediments. 22–32 cm. Yellowish–gray silty clay. 32–85 cm. Yellowish–gray clayey silt. Compact lacustrine sediments. There is clear horizontal bedding. 85–100 cm. Gray clayey silt. Lacustrine sediments with clear horizontal bedding. 100–140 cm. Gray clayey silt. Some plant fragments. 140–480 cm. Bluish gray clayey silt. Soft lacustrine sediments. A small wood is present at 448 cm. 480–580 cm. Gray–brown silty clay. Some 580–610 cm.
9	18SLH5	N30°08′36.84″, E121°19′42.69″	0–20 cm. Bluish gray clay. Soft lacustrine sediments. 20–80 cm. Yellowish brown clay. Abundant plant roots. Soft bog sediments. 80–300 cm. Bluish gray clayey silt. Some plant fragments. Soft lacustrine sediments. 300–580 cm. Yellowish–gray clayey silt. Some plant fragments. 580–800 cm. The gray–brown mixture of sand and mud. Soft texture. Some plant fragments. A small wood is present at 602 cm. Spiral shell fragments present at 667 cm, 691 cm, 751 cm, and 762 cm. Alluvial/eluvial sedimentary facies.
10	18SLH6	N30°07′50.43″ E121°19′46.36″	0–360 cm. Gray dark cultural layer with abundant rock, pottery pieces, and plant fragments. 360–400 cm. Gray silty clay. Compact lacustrine sediments. 400–435 cm. Yellowish brown and light gray clay. Compact paleosols.

Key Laboratory of Lake Science and Environment, Nanjing Institute of Geography and Limnology, Chinese Academy of Sciences, China.

The EMMA end element model method (Weltje, 1997) is able to distinguish between the different components of the grain size, running the Analysize package provided by Paterson and Heslop (2015) in the MATLAB environment. Since the bottom 30 cm of the cores is riverine sand, the particle size was calculated after excluding the bottom 15 samples. We chose three components with less information lost and a better correspondence with the distribution in the samples, namely, two single peak modes and a mode with one high and one low peak, labeled as EM1, EM2, and EM3, respectively (Figure 3).

2.3 TOC, TN and $\delta^{13}C$

The stable isotope composition of organic carbon is widely used as a proxy in paleoenvironmental reconstruction and can be used to quantify the relative proportions of marine versus terrestrially derived water and carbon in a range of sample materials (Bouillon et al., 2008), thus providing information on coastline proximity and hence sea level. Subsamples were taken from the core between 0–5.8 m depth for a total of 54 samples, to measure total organic carbon (TOC), total nitrogen (TN), and organic $\delta^{13}C$. TOC and TN were analyzed using an EA3000 Elemental Analyzer and organic $\delta^{13}C$ analysis were crushed and treated with acid in Ag-capsules prior to isotope analysis using a MAT251 elemental analyzer coupled in continuous flow mode to a Finnegan Delta Plus XL mass spectrometer (± 0.1‰ V-PDB), in the State Key Laboratory of Lake Science and Environment, Nanjing Institute of Geography and Limnology, Chinese Academy of Sciences, China.

2.4 Microfossil analyses

Microfossils, especially pollen, spores, freshwater algae, dinoflagellate cysts, and Foraminiferal organic linings as the most direct indicators or proxies, provide significant information on environmental evolution. Therefore, palynological analysis played an important role in restoration and reconstruction of vegetation history and sea-level fluctuations, which provides information from the sediment cores, especially in alluvial coastal plain regions. (Nakagawa et al., 2003; Pidek et al., 2010; Zhao et al., 2011; Lowe and Walker, 2015; Hao et al., 2022).

TABLE 2 Summary of radiocarbon dates obtained from cores.

Sample No.	Beta No.	Depth/cm	Material	^{14}C age	Calibrated age (cal. yr BP, 2σ range)
18SLH4-55	543783	55	Plant Material	4910±30	5665–5591
18SLH4-100	511659	100	Plant Material	6200±30	7179–7000
18SLH4-125	536113	125	Plant Material	6270±30	7265–7160
18SLH4-221	536114	221	Plant Material	6610±30	7566–7440
18SLH4-448	511658	448	Wood	6980±30	7872–7721
18SLH4-551	511660	551	Wood	7080±30	7965–7848
18SLH4-581	484449	581	Plant Material	7140±30	8015–7931
18SLH1-165	546022	165	Plant Material	5860±30	6749–6627
18SLH1-350	514643	350	Shell	6700±30	7618–7507
18SLH6-3A-96	514637	384	Plant Material	5170±30	5992–5896
18SLH5-568	514460	568	Plant Material	7060±30	7955–7839

Distributions of modern dinoflagellate cysts (dinocysts) and planktonic Foraminiferal fauna in marine environments are directly associated with upper water masses, sea-surface temperature, salinity, nitrate, phosphate, and other oceanographic variables (Rochon et al., 1999; Dale, 2009; de Vernal et al., 2005; Pospelova and Kim, 2010; Zonneveld et al., 2013; Hao et al., 2020). Therefore, organic-walled dinoflagellate cysts and foraminifer linings being preserved in sediments are commonly used as indicators for reconstructions of past sea-level fluctuations and oceanographic conditions (de Vernal et al., 2005; Zonneveld et al., 2008; Bringué et al., 2014; Pospelova et al., 2015).

In our study, subsamples every 3 cm were taken from the core of 18SLH4 between 0 and 1m, and at 10 cm intervals elsewhere, for a total of 83 samples for biological proxy analysis (palynology, Dinoflagellate cysts Foraminiferal organic linings). Samples were prepared for palynological analysis using the standard laboratory techniques, including alkali digestion, hydrofluoric acid digestion, and acetolysis (reference for pollen method here), but we didn't sieve at 180 μm to

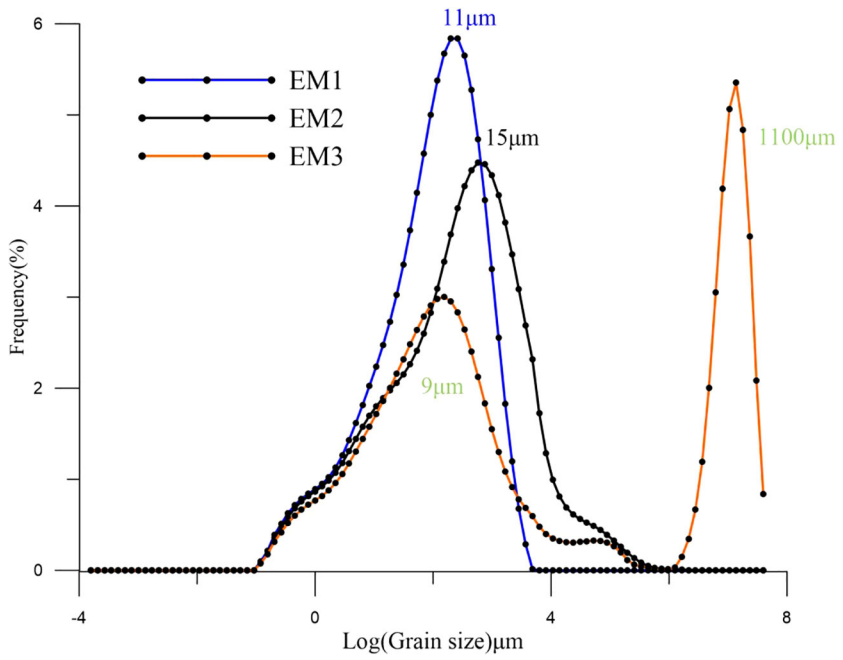

FIGURE 3
Distribution of End-Member of 18SLH4 from Shanglin Lake.

retain Foraminiferal linings. Microfossils were identified using reference keys and type slides and counted using a stereomicroscope at a magnification of ×400 for critical features. Identification of pollen grains, pteridophyte spores, and Foraminiferal organic linings followed He et al. (1965), Wang (1980), Wang et al. (1980), Wang et al. (2012) and Tang et al. (2019); Dinoflagellate cysts followed Moore et al. (1991), He et al. (2009) and Tang et al. (2013). 400 land pollen grains were counted for each sampled level, plus all aquatic pollen, pteridophyte spores, Dinoflagellate cysts and Foraminiferal organic linings.

3 Result

3.1 AMS^{14}C dating and age-depth model

The 11 ages include both original and tree-wheel corrected ages (Stuiver et al., 1993; Reimer et al., 2009) (http://calib.org, accessed in November 2016) (Table 2). A complete chronological framework was developed for the 18SLH4 core using the R package *Clam* (Figure 4).

3.2 Grain size analysis

Based on the lithological characteristics and dating results, 18SLH4 was selected for particle size testing, and a total of 265 samples were tested at equal intervals. The mean grain size of the cores was 6.93 μm, ranging from 4.22 to 7.93 μm (Figure 5).

The plural of the EM1 component is 11 μm, which is the main material input of the core, with an average value of 72.23%. The EM3, with the main peak at 1100 μm and the secondary peak at 9 μm, has a mean proportion of 3.36%, which may indicate the input of slope sediment and storm surge caused by abnormal floods.

3.3 Characteristics of TOC, TN and δ^{13}C

The records of TOC, TN, and δ^{13}C changes are given in Figure 6, and Figure 7 indicates the material sources of organic matter in the sediments for each period.

3.4 Microfossil assemblages

18SLH4 core found abundant spore pollen and microsomal paleontological fossils from nearly 100 families and genera, including regional arboreal pollen such as *Pinus, Fagus, Quercus, Cyclobalanopsis, Fagus, Betula, Carpinus, Corylus, Altingia, Ulmus, Juglans, Pterocarya*, Rosaceae, *Rhus*, etc.; pollen of endemic wet/aquatic herbs, such as *Phragmites, Suaeda*, Cyperaceae, *Typha, Nymphoides, Potamogeton*, etc.; pollen of herbs including Poaceae, Chenopodiaceae, Ranunculaceae, *Artemisia, Aster*, etc.; the spores of ferns including *Hicriopertis, Selaginella, Lycopodium, Pteris*, Sinopteridaceae, *Alsophila, Osnunda*, Hymenophyllaceae, Polypodiaceae, etc. There are also a variety of shallow marine

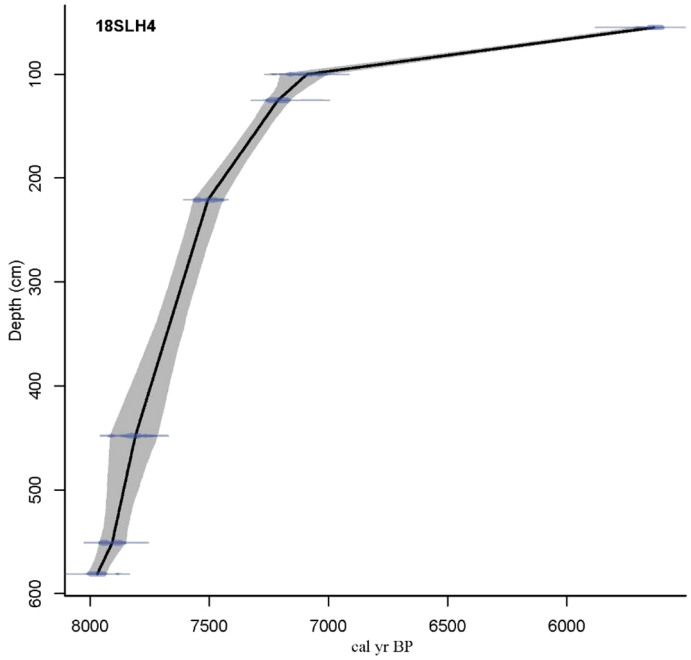

FIGURE 4
Lithology and age-depth model of 18SLH4 core from Shanglin Lake.

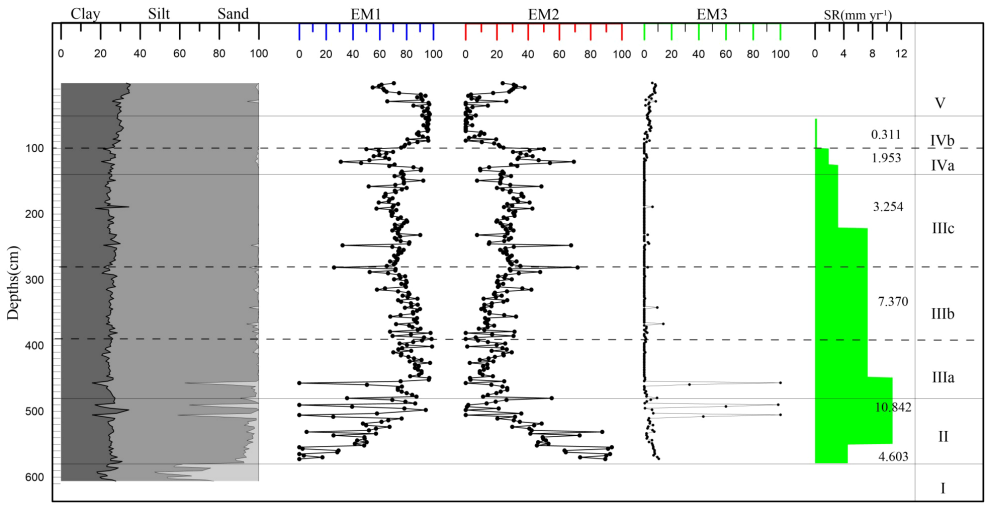

FIGURE 5
Vertical distribution of End-Member of the core 18SLH4 from Shanglin Lake.

Flagellates, such as *Multispinula, Spiniifertes, Operculodinium, Lingnlosphaeridium*, and *Selenopemphix*. *Polysphaeridium, Achomosphaera*, and a few freshwater algae such as *Zygnema, Pediastrum, Concentricyste*, etc. Two samples at 135 cm and 550 cm can be seen *Trochammina* and *Haplophragmoides* (*Trochammina* and *Haplophragmoides*, were identified under the guidance of Pro. Baohua Li, Nanjing Institute of Geology and Paleontology, Chinese Academy of Sciences), but a large number of Foraminiferal organic linings were found (Plates1–7).

Based on the comprehensive analysis of the content of the main spore pollen species and lithological characteristics combined with the clustering analysis of the terrestrial spore and pollen content, five zones can be classified from bottom to top (Figure 8, Figure 9).

Zone I (8031–7971 cal yr BP, 606–580 cm): The spore-pollen concentration is 6840 grains/ml on average. Pollen content of trees and shrubs (average 82.5%) is significantly higher than herbaceous pollen, dominated by deciduous *Quercus*, *Cyclobalanopsis*, and *Pinus*, of which, deciduous broad-leaved species accounted for about 43.7%, evergreen broad-leaved species accounted for 15.8%. The average pollen content of herbaceous plants reached 15.7%, mainly Poaceae (7.9%). The average content of fern spores was 14.6%; a small number of freshwater algae were found, no furrow flagellates were seen, and Foraminiferal organic linings were found

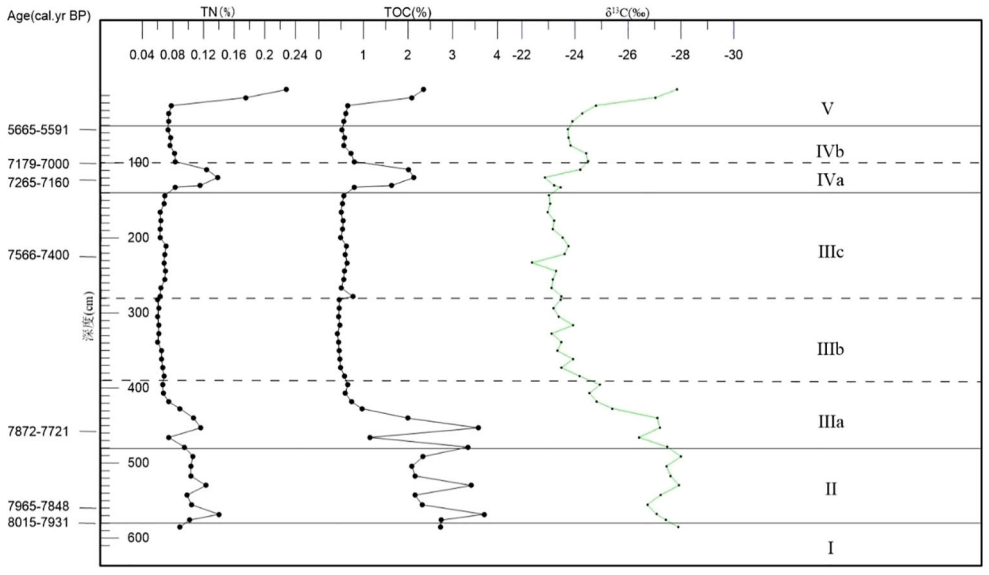

FIGURE 6
Vertical distribution of TOC, TN and $\delta^{13}C$ of the core 18SLH4 from Shanglin Lake.

10.3389/fevo.2023.1218658

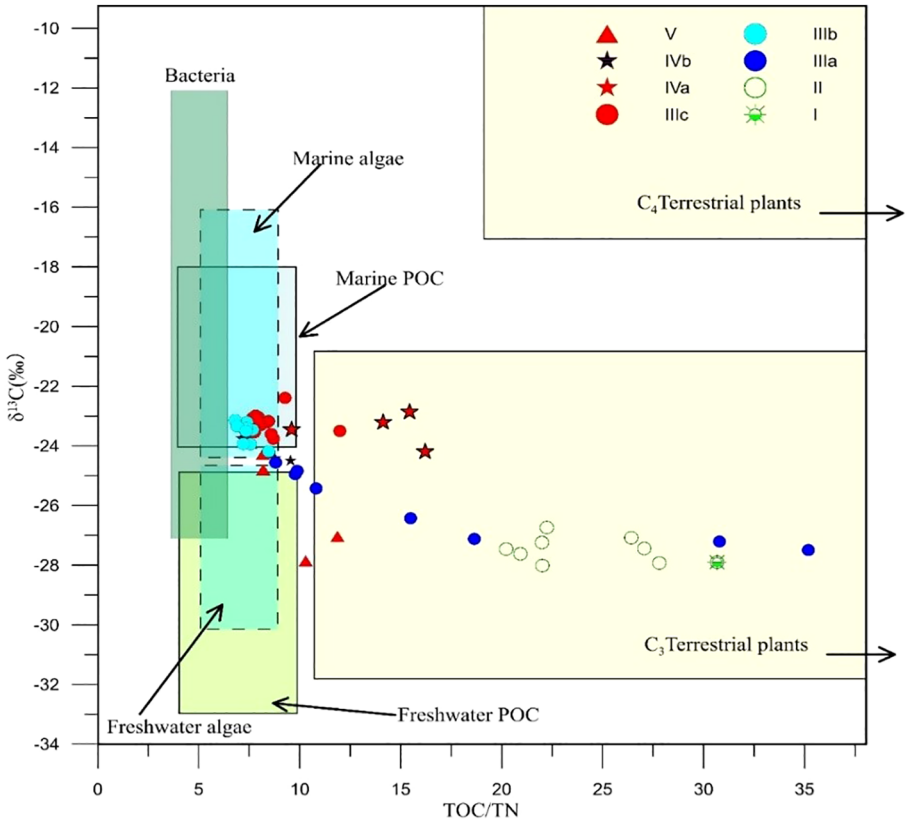

FIGURE 7
The source discrimination of organic carbon of the core 18SLH4 from Shanglin Lake (modified from Lamb et al., 2006).

with an endomorph of 363 grain/ml, mainly relatively fragmented individuals below 50 μm.

Zone II (7971–7848 cal yr BP, 580–480 cm): Spore-pollen concentration is 6704 grains/ml. Tree and shrub pollen dominates (average 80.5%), mainly deciduous *Quercus*, *Cyclobalanopsis*, and *pinus*, with 14.2% evergreen broad-leaved species. Herbaceous plants pollen accounts for an average of 16%, mainly Poaceae (8.6%). The average content of Cyperaceae is 3.6%; the average content of ferns is 15.3%, mainly in Hymenophyllaceae and Polypodiaceae, the average content of freshwater algae is less than

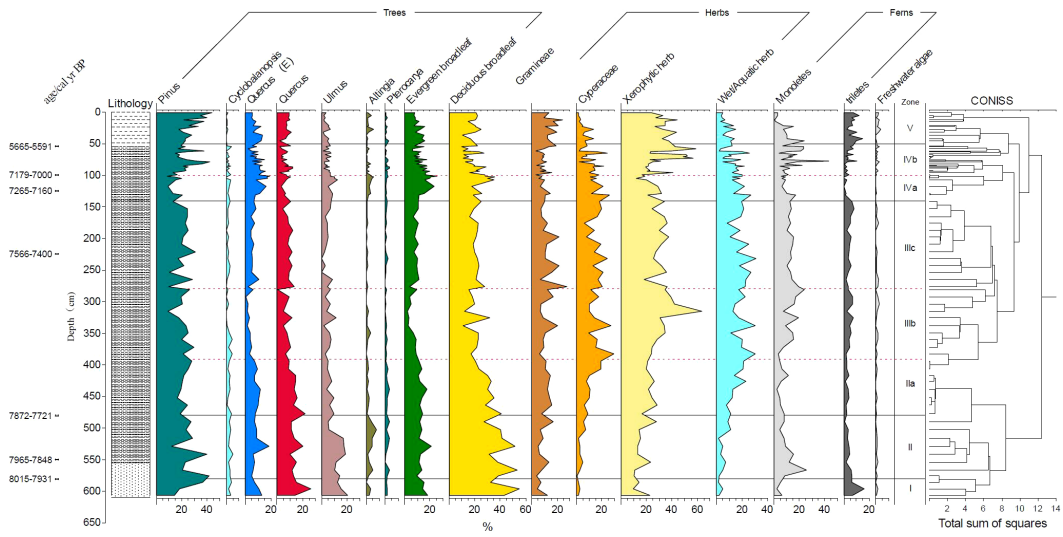

FIGURE 8
Pollen percent diagram of 18SLH4 from Shanglin Lake.

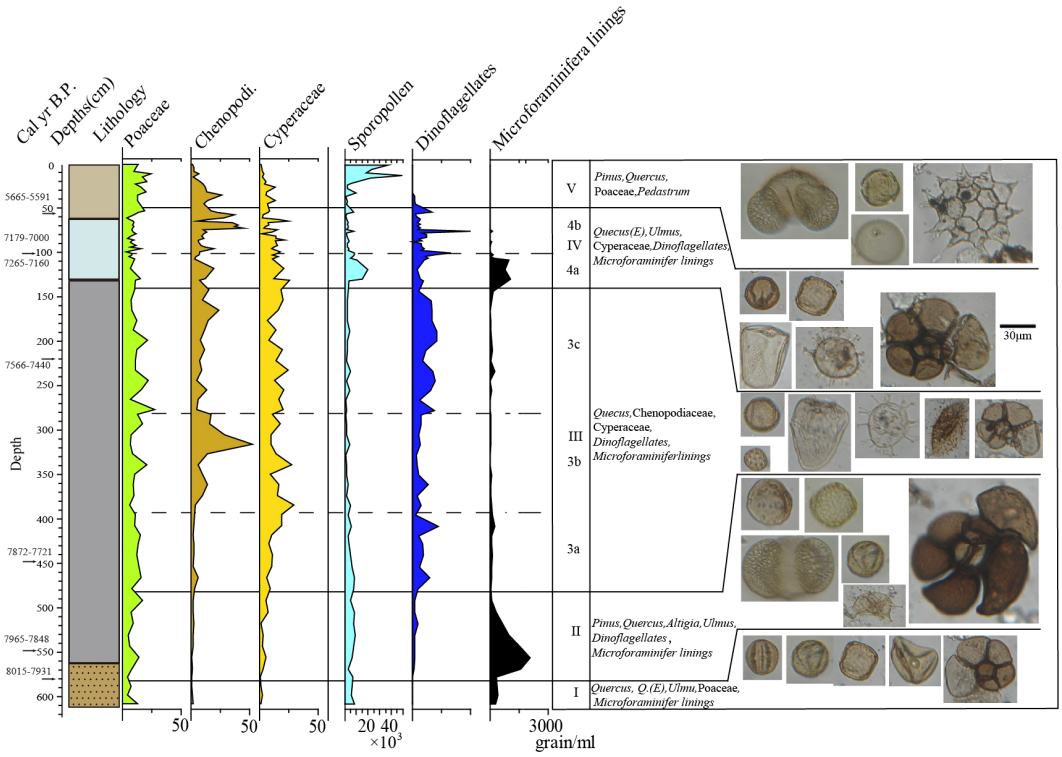

FIGURE 9
Multiproxy data of 18SLH4 from Shanglin Lake.

1%, and the average content of Dinoflagellate cysts is 37 grains/ml in the shallow/near-shore phase. At the same time, the Foraminiferal organic linings increase suddenly, with an average concentration of 1039 grains/ml, and a maximum of 2052 grains/ml. A small number of Foraminiferal shells could be seen.

Zone III (7848–7257 cal yr BP, 480–140 cm): The average concentration of spore pollen was 3960 grains/ml, which is the lowest stage of the whole core. The average pollen content of trees and shrubs was 53.64%, which dropped sharply compared with the previous two stages. The average content of Poaceae was 11.4%, Chenopodi was 10.4%, Cyperaceae was 12.6%, ferns was 15.8%, and the freshwater algae was less than 1%. The content of Dinoflagellate cysts began to increase at this stage, with an average content of 169 grains/ml. The content of Foraminiferal organic linings is extremely low, with an average of 74 grains/ml, mostly ranging in diameter from 50 to 100 μ m. At this stage, no Foraminiferal shell was found.

3a (7848–7735 cal yr BP, 480–390 cm): Pollen and spore concentration was 5343 grains/ml, which is the highest value in the whole of Zone 3, with 65% pollen content in trees and shrubs, 13.1% in Poaceae, 2.7% in Chenopodi, 11.8% in Cyperaceae with an increasing trend, reaching 19% at the end of the stage. 9% in ferns, 162 grains/ml in Dinoflagellate cysts. The concentration of Foraminiferal organic linings was 110 grains/ml.

3b (7735–7585 cal yr BP, 390–280 cm): The spore-pollen concentration was 1993 grains/ml, which is the lowest content in Zone III, with 46.78% of tree and shrub pollen, including 21% in Pinus, 10.6% in Poaceae and the average content of Chenopodiaceae is 17%, with a peak in the middle, with a maximum value of 52.3%, Cyperaceae of 16.2% with an upward trend. At the end of the stage, it reaches 19%, and ferns show a gradual upward trend. The average content is 18.4%, which is the highest content in cores. The content of Dinoflagellate cysts is 102 grains/ml, and the Foraminiferal organic linings are 46 grains/ml. Lowest for the entire Zone III.

3c (7585–7257 cal yr BP, 280–140 cm): The spore-pollen concentration was 2687 grains/ml, increasing compared to 3a, with 51.7% for arboreal pollen, 14.4% for Pinus, 10.6% for Poaceae, 17% for Chenopodi, with a peak in the middle and a maximum of 52.3%, 16.2% for Cyperaceae and 18.1% for ferns, with a relatively stable, with 236 grains/ml for the Dinoflagellate cysts, the highest stage of Zone III, and 80 grains/ml for the Foraminiferal organic linings.

Zone IV (7257–5567 cal yr BP, 140–50 cm): Spore-pollen concentration 4785 grains/ml, significantly increased compared with Zone III, pollen of trees and shrubs was 56.2%, pollen of *Pinus* was 21%, Poaceae was 8.9%, Chenopodi was 15.3%, Cyperaceae was 12.9%, fern was 15.5%, showing an increasing trend, freshwater algae was less than 1%, The content of Dinoflagellate cysts fluctuates greatly, the highest value is 161 grains/ml, was the highest stage of the whole profile, the Foraminiferal organic linings suddenly increases sharply, to the end stage of annihilation, the average is 156 grains/ml. The Foraminiferal shell is visible at this stage.

4a (7257–7082 cal yr BP, 140–100 cm): The spore-pollen concentration of 9806 grains/ml, a significant increase compared to the previous stage, pollen of tree shrubs was 66.6%, pollen of *Pinus* was 14.4%, a decrease, Poaceae was 8.9%, Chenopodi 15.3%, Cyperaceae 12.9%, ferns 15.5%, a slight increase compared to the previous stage, freshwater algae less than 1%, the concentration of Dinoflagellate cysts was 212 grains/ml, the average content of Foraminiferal organic linings in this stage was 593 grains/ml, and the highest stage was 1073 grains/ml, corresponding to the age of 7223 cal yr BP, showing a gradually decreasing trend. The spore-pollen was poorly preserved, and regional pollen of *Tsugar*, *Picea*, and *Abies* appeared.

4b (7082–5502 cal yr BP, 100–50 cm): The spore-pollen concentration 4785 grains/ml, a significant increase compared to the previous stage, tree and shrub pollen was 54.8%, *Pinus* pollen was 21%, Poaceae was 8.8%, Chenopodi was 8.5%, a significant decrease compared to 4a, Cyperaceae was 11.2%, fern was 17.2%, a slight increase compared to the previous a stage, freshwater algae was less than 1%, the concentration of Foraminiferal organic linings was 16 grains/ml on average, and the concentration was very low, but the location of 6278 cal yr BP showed a sudden change with a concentration of 151 grains/ml, and the concentration of Dinoflagellate cysts in this layer was the highest value in this stage.

Zone V (50–0 cm, 5502 cal yr BP–today): Spore-pollen concentration was 14631 grains/ml in the upper 20 cm, the average spore-pollen concentration was 30109 grains/ml, in the lower 30 cm the concentration was 3576 grains/ml, pollen of tree and shrubs was 59.6%, 64.5% in the upper part and 56.1% in the lower part, the average content of *pinus* was 29.1%, with the upper part being 35.5% in the upper part and 24.5% in the lower part. The content of Xerophytic herbs did not vary much, averaging 34.2%, Hygroscopic herbs showed a decreasing trend averaging 5.5%, with 2.3% in the upper part and 7.8% in the lower part, ferns varied more steadily, averaging 15.5%, and Poaceae varied more steadily averaging 15%.

The average content of Chenopodi was 9% and showed a decreasing trend in this zone with 2.8% in the upper part, the average content of Cyperaceae 5.5%, 2.2% in the upper part, 7.8%, and 13.4% in the lower part, showing a decreasing trend. Freshwater algae were 1.8% with less variation, no Dinoflagellate cysts was seen above the top 35 cm, and the average concentration at the bottom 15 cm was 35 grains/ml. No Foraminiferal organic linings were seen at this stage.

4 Discussions

4.1 Hydrological history of Shanglin Lake

4.1.1 Stage 1 (8031–7971 cal yr BP, 606–580 cm)

The Upper Forest Lake may be a paleo-valley during this time. The average content of sand reaches 37.36% with very poor sorting, and the sediments at the bottom of the paleo waterway SLH-2 and 18SLH5 core in the north are a mixture of silt and sand (Figure 2, Table 2), revealing strong hydrodynamics (Hori et al., 2002) TOC/TN and $\delta^{13}C$ scatter projections indicate that the source of organic matter is mainly terrestrial C3 vegetation (Lamb et al., 2006). The small amount of Foraminiferal organic linings and the absence of Dinoflagellate cysts were visible in this section, indicating sea level rise and the beginning of the Estuary stage (Zonneveld et al., 1997; Dale, 2009; Shennan, 2015).

4.1.2 Stage 2 (7971–7848 cal yr BP, 580–480 cm)

The sediment cores in this time period are gray-brown sandy silt. The EM2 is the highest stage in the whole core, with an average content of 45% and gradually decreasing from 89% at the bottom to 25% at the top, indicating strong marine wave energy. The EM3 end element indicates the possible presence of nearshore slope accumulation (Zhu, 2008). The content of Chenopodi is extremely low, averaging 1.4%, Poaceae averages 8.6%, and Cyperaceae averages 3.5%, and the combination with TOC/TN, $\delta^{13}C$ indicates that the source of organic matter is mainly terrestrial debris deposition from the watershed and ocean dynamics (Lamb et al., 2006). Dinoflagellate cysts gradually appeared but at low levels, and a large number of organic linings of varying individual sizes appeared in sediment samples, *Trochammina* were identified from this stage, revealing a relatively open marine environment with strong hydrodynamics, which was not conducive to the deposition of Dinoflagellate cysts, reflecting the rapid sea level rise at this stage (Bringué et al., 2014). Chenopodi and Cyperaceae showed a slow upward trend, indicating the development of the watershed flora towards the saline-alkali communities (Gao and Zhang, 2006; Wu et al., 2008; Tang et al., 2019). The concentrations of Foraminiferal organic linings showed a significant decreasing trend, indicating that sea level rise slowed at the end of this stage and the lagoons began to form.

4.1.3 Stage 3 (7848–7257 cal yr BP, 480–140 cm)

The grain-size characteristics of this stage are generally stable, and the physicochemical indexes are also stable, which means that the Shanglin Lake gradually enters a more stable lagoon stage, the lithology is dominated by greenish-gray muddy silt, and the TOC/TN, $\delta^{13}C$ reveals that the organic carbon is dominated by marine algae (Lamb et al., 2006); 3a (7848–7735 cal yr BP, 480–390 cm), TOC/TN, and $\delta^{13}C$ show a gradual transition from terrestrial to marine sources of organic carbon in the sediments (Lamb et al., 2006). With the influence of the gradual infiltration of seawater, the lake enters a rapid accumulation period, developing a variety of nearshore shallow marine phases of Dinoflagellate cysts, dominated by *Achomosphaera*, *Spiniifertes*, and *Operculodinium*, etc. The rapid rise in sea level makes the groundwater in the region saline and alkaline, and Wet herbaceous plants such as reeds, sedges, and suede on the lake beach were beginning to develop; 3b (7735–7585 cal yr BP, 390–280 cm), TOC/TN and $\delta^{13}C$ organic carbon are the sea source, but the concentration of flagellates appears low and seawater input decreases, at this time the sea level change was relatively stable or slightly decreasing, developing plant communities dominated by Quinoa, reeds, and sedge; 3c (7585–7257 cal yr BP, 280 cm), the sea level change is relatively stable or slightly decreasing, developing plant communities dominated by Quinoa, reeds and sedge. 7257 cal yr BP, 280–140 cm, the concentration of Dinoflagellate cysts increased, indicating sea level rise.

4.1.4 Stage 4 (7257–7082 cal yr BP, 140–100 cm)

In the early part of this stage, the sediments are black chalky silt, rich in plant remains containing woody debris, and a large number of benthic Foraminiferal organic linings (large) occur, which indicates that seawater is rapidly inundating the marsh, and thus this stage is a period of rapid sea level rise.

4.1.5 Stage 5 (7082–5502 cal yr BP, 100–50 cm)

The increase in freshwater algae, which indicates that lakeshore marshes are developing again, indicates that the sea level is in a more stable state. The presence of high levels of Chenopodi indicates the occurrence of salt marshes. At the depth of 75 cm, an abrupt change in the concentration of Dinoflagellate cysts at approximately 6278 cal yr BP was the maximum for this stage, as well as a small amount of Foraminiferal organic linings, suggesting a possible transient sea invasion at this location, as concluded in previous studies (Zheng et al., 2011; He et al., 2018; Wang et al., 2018; He et al., 2020).

4.1.6 Stage 6 (5502 cal yr BP–present day, 50–0 cm)

After ~5502 cal yr BP, the sediments have obvious horizontal stratification and are dominated by grayish-yellow chalky silt. The sporopollenin record shows the gradual disappearance of saline-tolerant plant species such as reeds, sedges, and suede, as well as the gradual disappearance of Dinoflagellate cysts, and the increase of *Typha*, along with the appearance of a small amount of Myriophyllum, which indicates that the lake of Shanglin Lake evolved into a freshwater lake.

4.2 The Mid-Holocene sea level fluctuations

Using 50 intertidal mangrove peat data and shallow marine sediments, Bird et al. (2007, 2010) reconstructed the sea level change in Singapore during 9.5–6.5 cal ka BP and concluded that sea level rose by 4 m during 7.5–7.0 cal kyr BP and slowly or stopped during 7.8 to 7.4 cal kyr BP in the Singapore area, but the rise was faster around that time. Wang et al. (2012) reconstructed the early-mid Holocene sea level change in the southern Yangtze River Delta and showed that it rose by about 2 m between 7.6 and 7.4 cal kyr BP.

The rapid rise of sea level in the early to Mid-Holocene, ~8000 cal yr BP seawater reached the foothills of the mountain slopes in the northern Ning Shao Plain (Liu et al., 2015; Zheng et al., 2018). Multiple indicators of Shanglin Lake reveal that ~8000 cal yr BP sea level reached the foothills of the Cixi area to form an estuarine bay, at which time the sediment elevation was about −5.6 m (Figure 2), and seawater began to inundate the lake connected to the ocean from this time. The period lasted until 7733 cal yr BP, after which the rate of rise slowed or even stopped. This means that the core was located near the coastal supratidal zone, and the sediment elevation at this time was −2.75 m (Figure 2). Thus, it can be inferred that the sea level rose rapidly from ~8000 cal yr BP to 7633 cal yr BP by about 3 m, and 7733–7585 cal yr BP was suitable for the survival of saline mudflats, with *Phragmites*, *Suaeda*, and Cyperaceae dominating the plant community. The low level of Dinoflagellate cysts relative to the pre-and post-phase indicates that the phase has been on the Supratidal Zone and the sea level rise stagnation lasted for nearly 150 years, after which the sea level started to enter the rising phase (7585–7082 cal yr BP), which is consistent with Bird et al. (2007) who suggested that the sea level stagnated or even slightly decreased from 7.8–7.4 cal kyr BP and the pattern of rapid sea level rise around that time is similar, but there are some differences in the timing and duration of the occurrence in this study.

From ~7585 cal yr BP, the saline plant community of Shanglin Lake started to fall, and the sea level was about −2.75 m. The sediment of ~7253 cal yr BP was deposited nearshore and shallow, and the sea level was about −1.35 m as inferred from the elevation of the sediment at this time. About 300 years later, the sea level rose about 1.4 m, and Shanglin Lake was connected to the sea again. After that, until ~7082 cal yr BP, the sea level was relatively stable and maintained a high sea level for nearly 200 years.

After ~7000 cal yr BP, the concentration of Foraminiferal organic linings fell back to low values and disappeared rapidly, and the saline plant community gradually developed to dominate again. Shanglin Lake begins to break away from the direct influence of the ocean, implying the end of the high sea level period, and drops back to close to modern sea level. Sediment elevations during this time period approached modern sea level elevations. The dominance of saline plant communities during ~7000–5500 cal yr BP indicates that coastal areas at 0–1 m elevation in the Ning Shao Plain area have been in the supratidal zone during this time period. There were also several peaks in the concentration of trench whip algae during this time, indicating the influence of sea level fluctuations, including (Figure 9) a peak in the concentration of trench whip algae at ~6278 cal yr BP at 75 cm, as well as a small amount of Foraminiferal organic linings, suggesting that a sea invasion may have occurred at this time.

Multi-indicator analysis of high-resolution sediments from the 18SLH4 core in Shanglin Lake reveals that sea level in the Ningshao Coastal Plain varies minimally or decreases slightly from ~7733–7585 cal yr BP, with a rapid sea level rise around this period and a high sea level at ~7253–7082 cal yr BP. Between ~7000–5500 cal yr BP, sea level is more stable with small fluctuations, with a brief sea intrusion at ~6280 cal yr BP.

4.3 Sea level changes and cultural history

Early rice cultivation from 7700 cal yr B.P. has recently been demonstrated from the Yangtze delta at Kuahuqiao, which site was abandoned due to renewed sea-level rise ca. 7550 cal yr BP (Zong et al., 2007; Innes et al., 2009). Several previous studies have shown that the region was detached from seawater influence at about 7600 cal yr BP, and coastal wetlands began to form in the foothills of the plains during 7500–7000 cal a BP (Dai et al., 2018; Liu et al., 2018). The plant communities revealed by the spore-pollen of Shanglin Lake show that the region developed coastal wetlands at 7733–7585 cal yr BP, with a peak at about 7600 cal B.P, after which the sea did not recede and the sea level continued

to grow. At 7253–7082 cal yr BP, sea level rose rapidly to form a semi-enclosed bay environment, appearing nearly 200 years in subtidal lagoonal phase deposition.

The sea level after 7000 cal yr BP began to fall back until 5502 cal yr BP, when supratidal ecological communities with absolute dominance of Phragmites, *Suaeda*, and Cyperaceae, indicating that the sea level maintained a stable and slightly fluctuating environment, making the early Hemudu and Tianluoshan cultures less prosperous than the Majiabang and Songze cultures in northern Hangzhou Bay. The relative survival pressure of the Hemudu and Tianluoshan people was higher (Qin et al., 2011). The extreme peak of Dinoflagellate cysts at about 6278 cal yr BP, along with a small amount of Foraminiferal organic linings, indicates a brief sea invasion during this period, which is consistent with the sea invasion event of 6400–6300 cal yr BP derived from previous studies. Seed analysis shows that the time of sea invasion from 6400 to 6300 cal yr BP was recorded (Zheng et al., 2012). The presence of moderate amounts of Dinoflagellate cysts in samples between about 6278 cal yr BP and about 5600 cal yr B.P. indicates that seawater had been influencing ancient human activities in the Ningshao Plain area during this period, and that saline plant communities were more developed at this stage, suggesting that the Hemudu people lived in relatively saline groundwater conditions for agricultural activities at that time. Multi-indicator analysis of the Yushan site (Figure 1A) by He et al. (2018) showed that the Hemudu culture 6300–5600 was interrupted by transgression, but Wang et al. (2012) infer that extreme events and flooding accompanying accelerated sea-level rise were major causes of cultural interruption. However, the sediments of this phase in Shanglin Lake have more obvious stratification and no obvious storm surge accumulation features.

5 Conclusion

We selected Shanglin Lake, which is surrounded by mountains on three sides and faces Hangzhou Bay in the back north, away from the alluvial plain and disturbed by river alluvium, to reconstruct a detailed history of sea level changes in the Cixi region of Zhejiang from 8–5.6 cal yr BP based on a well-established chronosequence and multiple proxies such as grain size, TOC/TN, $\delta^{13}C$, sporo-pollen, Dinoflagellate cysts, Foraminiferal organic, etc.

Our study indicated that the evolution of Shanglin Lake since the Mid-Holocene experienced the stages of the estuarine bay, semi-enclosed bay, semi-enclosed lagoon, semi-enclosed bay, enclosed lagoon, and modern lake.

The multiple proxies suggest that there was a period of no or minimal eustatic sea-level rise between 7733 and 7585 cal yr BP in Ningshao Coastal Plain, Yangtze River Delta region. The Mid-Holocene high sea level comes in 7253–7082 cal yr BP. Between 7000 cal yr BP and 5502 cal yr BP, the sea level is relatively stable and fluctuates around modern height.

The sea level changes may directly influence the Neolithic cultural transitions in the Mid-Holocene in the Ningshao plain, which provides warnings for predicting the possible impacts of coastal deltas in response to sea level rise in the context of global warming.

Data availability statement

The original contributions presented in the study are included in the article/Supplementary Material. Further inquiries can be directed to the corresponding author.

Author contributions

CL: writing – original draft, validation, resources, and formal analysis. LT and BX: contributed to the conceptualization of the study. CL and SY: investigation and fieldwork. BX: supervision. CL, WZ, and DP revised the manuscript. All authors contributed to the article and approved the submitted version.

Funding

This research has been supported by, the Natural Science Foundation of Fujian Province (grant no. 2022J05178) and the Natural Science Foundation of Hunan Province (grant no. 2021JJ30555).

Acknowledgments

We are very grateful to Prof. Baohua Li (Nanjing Institute of Geology and Paleontology, Chinese Academy of Sciences) for his help in the identification of foraminifera fossils. Jingkui Tao and Wei Wang from Nanjing Institute of Geography and Limnology, Chinese Academy of Sciences are thanked for their hard work during the field campaign.

Conflict of interest

The authors declare that the research was conducted in the absence of any commercial or financial relationships that could be construed as a potential conflict of interest.

Publisher's note

Supplementary material

The Supplementary Material for this article can be found online at: https://www.frontiersin.org/articles/10.3389/fevo.2023.1218658/full#supplementary-material

References

Beuselinck, L., Govers, G., Poesen, J., Degraer, G., and Froyen, L. (1998). Grain-size analysis by laser diffractometry: comparison with the sieve-pipette method. *Catena* 32, 193–208. doi: 10.1016/S0341-8162(98)00051-4

Bird, M. I., Austin, W. E. N., Wurster, C. M., Fifield, L. K., Mojtahid, M., Sargeant, C., et al. (2010). Punctuated eustatic sea-level rise in the early Mid-Holocene. *Geology* 38 (9), 803–806. doi: 10.1130/G31066.1

Bird, M. I., Fifi eld, L. K., Chang, C. H., Teh, T. S., and Lambeck, K. (2007). An infl ection in the rate of early Mid-Holocene sea-level rise: A new sea-level curve for Singapore. *Estuar Coast Shelf Sci.* 71, 523–536. doi: 10.1016/j.ecss.2006.07.004

Bouillon, S., Connolly, R., and Lee, S. Y. (2008). Organic matter exchange and cycling in mangrove ecosystems: Recent insights from stable isotope studies. *J. Sea Res.* 59, 44–58. doi: 10.1016/j.seares.2007.05.001

Bringué, M., Pospelova, V., and Field, D. B. (2014). High resolution sedimentary record of dinoflagellate cysts reflects decadal variability and 20th century warming in the Santa Barbara Basin. *Quat. Sci. Rev.* 105, 86–101. doi: 10.1016/j.quascirev.2014.09.022

Chen, Q., Lu, Y., and Le, Z. (1984). On the lacustrine fluctuation in the regions of Ningbo-Shaoxing Plain in historical periods (in Chinese with English abstract). *Geo. Res.* 3 (3), 29–43.

Chen, Z., and Stanlety, D. J. (1998). Sea-Level rise on eastern China's Yangtze delta. *J. Coast. Res.* 14 (1), 360–366. http://www.jstor.org/stable/4298785.

Chen, Z., Wang, Z., Schneiderman, J., Taol, J., and Cail, Y. (2005). Holocene climate fluctuations in the Yangtze delta of eastern China and the Neolithic response. *Holocene* 15 (6), 915–924. doi: 10.1191/0959683605hl862rr

Dai, B., Liu, Y., Sun, Q., Zhang, W., and Chen, Z. (2018). Foraminiferal evidence for the Holocene environmental transitions in the Yaojiang Valley, south Hangzhou Bay of eastern China and its Neolithic implications. *Mar. Geology* 404, 15–23. doi: 10.1016/j.margeo.2018.07.001

Dale, B. (2009). Eutrophication signals in the sedimentary record of dinoflagellate cysts in coastal waters. *J. Sea Res.* 61 (1-2), 103–113. doi: 10.1016/j.seares.2008.06.007

de Vernal, A., Eynaud, F., Henry, M., Hillaire-Marcel, C., Londeix, L., Mangin, S., et al. (2005). Reconstruction of sea-surface conditions at middle to high latitudes of the Northern Hemisphere during the Last Glacial Maximum (LGM) based on dinoflagellate cyst assemblages. *Quaternary Sci. Rev.* 24, 897–924. doi: 10.1016/j.quascirev.2004.06.014

Feng, H., and Wang, Z. (1986). Zhejiang's holocene coastline shift and sea-level change (in Chinese with English abstract). *J. Hangzhou Univ.* 13 (01), 100–107.

Fuller, D. Q. (2007). Contrasting patterns in crop domestication and domestication rates: recent archaeobotanical insights from the old world. *Ann. Bot.* 100 (5), 903–924. doi: 10.1093/aob/mcm048

Fuller, D. Q. (2011). Pathways to Asian civilizations: tracing the origins and spread of rice and rice cultures. *Rice* 4 (3-4), 78–92. doi: 10.1007/s12284-011-9078-7

Fuller, D. Q., Ling, Q., Zheng, Y. F., Zhao, Z. J., Chen, X. G., Hosoya, L. A., et al. (2009). The domestication process and domestication rate in rice: spikelet bases from the Lower Yangtze. *Science* 323, 1607–1610. doi: 10.1126/science.1166605

Gao, Z., and Zhang, L. (2006). Measuring and analyzing of the mult-i seasonal spectral characteristics for saltmarsh vegetation in shanghai (in chinese with english abstract). *Acta Ecologica Sin.* 26 (3), 793–800.

Hao, X., Li, L., Ouyang, X., Qin, L., Jiang, X., Li, J., et al. (2022). Holocene vegetation evolution, hydrologic variability and sea-level fluctuations on the south coastal plain of Laizhou Bay, Bohai Sea, China: new evidence from pollen, freshwater algae and dinoflagellate cysts. *J. Paleolimnol* 68, 155–167. doi: 10.1007/s10933-021-00229-2

Hao, X., Ouyang, X., Zheng, L., Zhuo, B., and Liu, Y. (2020). Palynological evidence for Early to Mid-Holocene sea-level fluctuations over the present-day Ningshao Coastal Plain in eastern China. *Mar. Geology* 426, 106213. doi: 10.1016/j.margeo.2020.106213

He, C., Song, Z., and Zhu, Y. (2009). *Fossil dinoflagellates of china (in chinese)* (Beijing: Science Press).

He, Y., Hu, L. Y., and Wang, K. L. (1965). Quaternary Foraminiferal in the east region of Jiang-su Province. Memoirs of Nanjing Institute of Geology and Palaeontology. *Chin. Acad. Sci.* 4, 51–162.

He, K., Lu, H., Li, Y., Ding, F., Zhang, J., and Wang, C. (2020). Cultural response to Middle Holocene sea-level fluctuations in eastern China: a multi-proxy approach. *Boreas* 49 (1), 71–88. doi: 10.1111/bor.12421

He, K., Lu, H., Zheng, Y., Zhang, J., Xu, D., Huang, X., et al. (2018). Middle-Holocene sea-level fluctuations interrupted the developing Hemudu culture in the lower Yangtze River, China. *Quaternary Sci. Rev.* 188, 90–103. doi: 10.1016/j.quascirev.2018.03.034

Hori, K., Saito, Y., and Wang, P. (2002). Evolution of the coastal depositional systems of the changjiang (Yangtze) river in response to late pleistocene-holocene sea-level changes[J]. *J. Sedimentary Res.* 2002, 72.

Innes, J. B., Zong, Y., Chen, Z., Chen, C., Wang, Z., and Wang, H. (2009). Environmental history, palaeoecology and human activity at the early neolithic forager/cultivator site at kuahuqiao, hangzhou, eastern china. *Quaternary Sci. Rev.* 28 (23-24), 2277–2294. doi: 10.1016/j.quascirev.2009.04.010

Innes, J. B., Zong, Y., Xiong, H., Wang, Z., and Chen, Z. (2019). Pollen and non-pollen palynomorph analyses of Upper Holocene sediments from Dianshan, Yangtze coastal lowlands, China: Hydrology, vegetation history and human activity. *Palaeogeogr. Palaeoclimatol. Palaeoecol.* 523, 30–47. doi: 10.1016/j.palaeo.2019.03.009

Lamb, A. L., Wilson, G. P., and Leng, M. J. (2006). A review of coastal palaeoclimate and relative sea-level reconstructions using [delta] 13c and c/n ratios in organic material. *Earth Sci. Rev.* 75 (1-4), 29–57. doi: 10.1016/j.earscirev.2005.10.003

Li, Z., Song, B., Saito, Y., and Li, J. (2009). "Sedimentary facies and geochemical characteristics of Jiangdou Core JD01 from the upper delta plain of Changjiang (Yangtze) delta, China," in *Ias Meeting of Sedimentologists*.

Liu, Y., Sun, Q., Fan, D., Lai, X., Xu, L., Finlayson, B., et al. (2016). Pollen evidence to interpret the history of rice farming at the Hemudu site on the Ningshao coast, eastern China. *Quaternary Int.* 426 (dec.28), 195–203. doi: 10.1016/j.quaint.2016.05.016

Liu, Y., Sun, Q., Fan, D., Dai, B., Ma, F., Xu, L., et al. (2018). Early to Middle Holocene sea level fluctuation, coastal progradation and the Neolithic occupation in the Yaojiang Valley of southern Hangzhou Bay, Eastern China. *Quaternary Sci. Rev.* 189, 91–104. doi: 10.1016/j.quascirev.2018.04.010

Liu, Y., Sun, Q., Thomas, I., et al. (2015). Middle holocene coastal environment and the rise of the liangzhu city complex on the yangtze delta, china. *Quaternary Res.* 84 (3), 326–334. doi: 10.1016/j.yqres.2015.10.001

Liu, X., Liu, Z., Qian, Q., Song, W., Yuan, Y., et al. (2020). Isotope chemometrics determines farming methods and geographical origin of vegetables from yangtze river delta region, china. *Food Chem.* 342, 128379. doi: 10.1016/j.foodchem.2020.128379

Lowe, J., and Walker, M. (2015). *Reconstructing quaternary environments. 3rd edn* (New York, USA: Routledge), 183–197.

Moore, P. D., Webb, J. A., and Collison, M. E. (1991). *Pollen Analysis* (London: Blackwell Scientific Publications), 127–131.

Nakagawa, T., Kitagawa, H., Yasuda, Y., Tarasov, P., Nishida, K., Gotanda, K., et al. (2003). Asynchronous climate changes in the North Atlantic and Japan during the last termination. *Science* 299, 688–691. doi: 10.1126/science.1078235

Ningbo Chorography Codification Committee (1995). *Ningbo Chorography* (Beijing: Zhonghua Book Company).

Paterson, G. A., and Heslop, D. (2015). New methods for unmixing sediment grain size data. *Geochemistry* 16 (12), 4494–4506. doi: 10.1002/2015GC006070

Pidek, I., Piotrowska, K., and Kasprzyk, I. (2010). Pollen-vegetation relationships for pine and spruce in southeast Poland on the basis of volumetric and Tauber trap records. *Gran* 49, 215–226. doi: 10.1080/00173134.2010.514006

Pospelova, V., and Kim, S. J. (2010). Dinoflagellate cysts in recent sediments from the aquaculture sites of southern South Korea. *Mar. Micropaleontol.* 76, 37–51. doi: 10.1016/j.marmicro.2010.04.003

Pospelova, V., Price, A., and Pedersen, T. (2015). Palynological evidence for late quaternary climate and marine primary productivity changes along the California margin. *Paleoceanography* 30, 877–894. doi: 10.1002/2014PA002728

Qin, J., Taylor, D., Atahan, P., Zhang, X., Wu, G., Dodson, J., et al. (2011). Neolithic agriculture, freshwater resources and rapid environmental changes on the lower Yangtze, China. *Quaternary Res.* 75 (1), 55–65. doi: 10.1016/j.yqres.2010.07.014

Reimer, P. J., Baillie, M. G. L., Bard, E., Bayliss, A., Beck, J., Blackwell, P., et al. (2009). IntCal09 and Marine09 radiocarbon age calibration curves, 0–50,000 years cal. BP. *Radiocarbon* 51, 1111–1150. doi: 10.1017/S0033822200034202

Rochon, A., de Vernal, A., Turon, J.-L., Matthiessen, J., and Head, M. J. (1999). Distribution of recent dinoflagellate cysts in surface sediments from the north atlantic ocean and adjacent areas in relation to sea-surface parameters. *Am. Assoc. Stratigraphic Palynologists Contributions Ser.* 35, 146.

Sandweiss, D. H. (2003). Terminal Pleistocene through Mid-Holocene archaeological sites as paleoclimatic archives for the Peruvian coast. *Palaeogeogr. Palaeoclimatol. Palaeoecol.* 194 (1-3), 23–40. doi: 10.1016/S0031-0182(03)00270-0

Shennan, I. (2015). *Handbook of sea-level research* (Wiley-Blackwell). doi: 10.1002/9781118452547.ch2

Shu, J., Wang, W., Jiang, L., and Takahara, H. (2010). Early Neolithic vegetation history, fire regime and human activity at Kuahuqiao, Lower Yangtze River, East China: New and improved insight. *Quaternary Int.* 227 (1), 10–21. doi: 10.1016/j.quaint.2010.04.010

Silva, F., Stevens, C. J., Weisskopf, A., Cristina, C., Ling, Q., Andrew, B., et al. (2015). Modelling the geographical origin of rice cultivation in asia using the rice archaeological database. *PLoS One*. doi: 10.1371/journal.pone.0137024

Song, B., Li, Z., Saito, Y., Okuno, J., Lu, A., Hua, D., et al. (2013). Initiation of the Changjiang (Yangtze) delta and its response to the Mid-Holocene sea level change. *Palaeogeography Palaeoclimatology Palaeoecol.* 388, 81–97. doi: 10.1016/j.palaeo.2013.07.026

Stuiver, M., Reimer, P. J., and Reimer, R. W. (1993). Extended C-14 data-base and revised Calib 7.1 C-14age calibration program. *Radiocarbon* 35, 215–230.

Tang, L., Shu, J., Chen, J., and Wang, Z. (2019). Mid to late Holocene vegetation change recorded at a Neolithic site in the Yangtze coastal plain, China. *Quaternary Int.* 59, 122–130. doi: 10.1016/j.quaint.2018.12.031

Tang, L. Y., Mao, L. M., Lu, X., Ma, Q., Zhou, Z. Z., Yang, C. L., et al. (2013). Palaeoecological and palaeoenvironmental significance of some important spores and micro-algae in quaternary deposits. *Chin. Sci. Bull.* 58, 3125–3139. doi: 10.1007/s11434-013-5747-9

Wang, P. X. (1980). *Collection of Papers on Marine Microfossil* (Beijing: China Ocean Press), 1–204.

Wang, P. X., Min, Q. B., Bian, Y. H., and Zhang, J. J. (1980). Micropaleontologic characteristics of relict sediments of the East China sea. *(in Chinese with English abstract) Acta Oceanologia Sin.* 2 (1), 67–78.

Wang, P. X. (1982). The changes of sea-level in Holocene on the coast of Zhejiang (in Chinese with English abstract). *Mar. Geo. Res.* 2 (2), 79–88.

Wang, Z., Ryves, D. B., Lei, S., et al. (2018). Middle Holocene marine flooding and human response in the south Yangtze coastal plain, East China. *Quaternary Sci. Rev.* 187, 80–93. doi: 10.1016/j.quascirev.2018.03.001

Wang, Z., Zhuang, C., Saito, Y., et al. (2012). Early Mid-Holocene sea-level change and coastal environmental response on the southern Yangtze delta plain, China: implications for the rise of Neolithic culture. *Quaternary Sci. Rev.* 35 (none), 51–62. doi: 10.1016/j.quascirev.2012.01.005

Weltje, G. J. (1997). End-member modeling of compositional data: numerical-statistical algorithms for solving the explicit mixing problem. *Math. Geology* 29 (4), 503–549. doi: 10.1007/BF02775085

Wu, Z. Y. (1980). Vegetation of China. (Beijing: Science Press).

Wu, T., Wu, M., and Xiao, J. (2008). Dynamics of community succession and species diversity of vegetations in beach wetlands of hangzhou bay (in chinese with english abstract). *Chin. J. Ecol.* 27 (8), 1284–1289.

Xie, Z. R., and Yuan, L. W. (2012). Fluctuation characteristics of Holocene sea-level change and its environmental implications. *Quaternary Sci.*

Zhao, Z. J. (2010). New data and new issues for the study of origin of rice agriculture in China. *Archaeological Anthropological Sci.* 2 (2), 99–105. doi: 10.1007/s12520-010-0028-x

Zhao, Z. J. (2019). Introduction of the origin of agriculture in China. *Res. Heritages Preserservation* 4 (1), 1–7.

Zhao, Y., Yu, Z., and Zhao, W. (2011). Holocene vegetation and climate histories in the eastern Tibetan Plateau: controls by insolation- driven temperature or monsoon-derived precipitation changes? *Quat Sci. Rev.* 30, 1173–1184. doi: 10.1016/j.quascirev.2011.02.006

Zheng, H., Zhou, Y., Yang, Q., Hu, Z., Ling, G., Zhang, J., et al. (2018). Spatial and temporal distribution of Neolithic sites in coastal China: Sea level changes, geomorphic evolution and human adaption. *Sci. China Earth Sci.* 61, 123–133. doi: 10.1007/s11430-017-9121-y

Zheng, Y. F., Sun, G. P., and Chen, X. G. (2011). Response of rice cultivation to fluctuating sea level during the Mid-Holocene. *Chin. Sci. Bull.* 56, 2888 ~ 2896. doi: 10.1007/s11434-011-4786-3

Zheng, Y., Sun, G., and Chen, X. (2012). Response of rice cultivation to fluctuating sea level during the mid-holocene. *Chin. Sci. Bull.* 57, 370–378. doi: 10.1007/s11434-011-4786-3

Zhu, C., Zheng, C. G., Ma, C. M., Yang, X., Gao, X., Wang, H., et al. (2003). On the Holocene sea-level highstand along the Yangtze Delta and Ningshao Plain, east China [J]. *Chin. Sci. Bull.* 48 (24), 2672–2683. doi: 10.1007/BF02901755

Zhu, X. (2008). *) sedimentary petrology (in chinese)* (Beijing: Petroleum Industry Press).

Zonneveld, K. F., Versteegh, G. J. M., and Lange, G. J. D. (1997). Preservation of organic-walled dinoflagellate cysts in different oxygen regimes: a 10,000 year natural experiment. *Mar. Micropaleontology* 29, 393–405. doi: 10.1016/S0377-8398(96)00032-1

Zong, Y. (2004). Mid-Holocene sea-level highstand along the Southeast Coast of China. *Quaternary Int.* 117 (1), 55–67. doi: 10.1016/S1040-6182(03)00116-2

Zong, Y., Chen, Z., Innes, J. B., Chen, C., Wang, Z., and Wang, H. (2007). Fire and flood management of coastal swamp enabled first rice paddy cultivation in east China. *Nature* 449, 459–462. doi: 10.1038/nature06135

Zong, Y., Wang, Z., Innes, J. B., and Chen, Z. (2011). Holocene environmental change and Neolithic rice agriculture in the lower Yangtze region of China: A review. *Holocene* 22 (6), 623–635. doi: 10.1177/0959683611409775

Zonneveld, K. A. F., Marret, F., Versteegh, G. J. M., Bogus, K., Bonnet, S., Bouimetarhan, I., et al. (2013). Atlas of modern dinoflagellate cyst distribution based on 2405 data points. *Rev. Palaeobot. Palynol.* 191, 1–197. doi: 10.1016/j.revpalbo.2012.08.003

Zonneveld, K., Versteegh, G., and Kodrans-Nsiah, M. (2008). Preservation and organic chemistry of late Cenozoic organicwalled dinoflagellate cysts: a review. *Mar. Micropaleontol* 68, 179–197. doi: 10.1016/j.marmicro.2008.01.015